Synthesis, X-ray Structure, and Physical and Photophysical Properties of the Heterobimetallic Complex Fe(η^5-$C_5H_4PPh_2$)$_2$Pt(bph)

Greg Y. Zheng,[†] D. Paul Rillema,*[,†] and Joseph H. Reibenspies[‡]

Departments of Chemistry, Wichita State University, Wichita, Kansas 67260-0051, and Texas A & M Univesity, College Station, Texas 77843-3255

Received May 15, 1998

A chromophore-electroactive compound, Fe(η^5-$C_5H_4PPh_2$)$_2$Pt(bph), where bph is the biphenyl dianion and Fe(η^5-$C_5H_4PPh_2$)$_2$ is 1,1′-bis(diphenylphosphino)ferrocene-*P*,*P*′ has been synthesized. The single-crystal X-ray structural characteristics of this heterobimetallic complex and its disolvated methylene chloride derivative are respectively as follows: empirical formula $C_{46}H_{36}FeP_2Pt$, triclinic, $P\bar{1}$, $Z = 4$, $a = 9.777(2)$ Å, $b = 18.003(4)$ Å, $c = 20.882(4)$ Å, $\alpha = 93.57(3)°$, $\beta = 100.99(3)°$, and $\gamma = 90.86(3)°$, and empirical formula $C_{48}H_{40}Cl_2FeP_2Pt$, monoclinic, $P2_1/n$, $Z = 4$, $a = 12.698(3)$ Å, $b = 14.161(3)$ Å, $c = 23.376(6)$ Å, $\alpha = 90°$, $\beta = 94.107(14)°$, and $\gamma = 90°$. An electrochemical study shows that the anodic potential for the oxidation of the ferrocenyl moiety of this compound increases by +0.13 V, compared to that for Fe(η^5-$C_5H_4PPh_2$)$_2$. This change in oxidation potential agrees well with the change in energy of 0.11 eV for the dπ(Fe) → π*(Cp) MLCT transition upon coordination with Pt. The resultant excited state from the dπ(Pt) → π*(bph) MLCT transition is readily quenched by the ferrocenyl moiety unit as expected, and charge-separated redox-active centers are formed.

Introduction

With respect to solar energy conversion such as photoinduced water splitting, a currently active research field is the design and synthesis of chromophore-electroactive quencher systems in which physical separation of oxidation and reduction catalytic sites is obtained. The ferrocenyl moiety, which is a redox-active electron donor unit, appears to be an active candidate for incorporation into a chromophore unit, such as Ru, Re, and Pt complexes.[1−3]

In the past few years, the synthesis of several Pt(II) complexes has been carried out in our research group in order to search for good candidates for photocatalysis capable of solar energy conversion.[4−9] We have found that Pt(bph)(CO)$_2$ has served as a good intermediate for synthesizing other derivatives.[7] Since the derivatives having Pt(II) bonded to the biphenyl dianion showed strong emission in solution, which is attributed to a metal-perturbed bph-centered ^{3}LC state, a bimetallic complex containing a Pt(bph) and a ferrocene unit was constructed as a good candidate for examining charge separation processes induced photochemically. We report here the synthesis of a 1,1′-bis(diphenylphosphino)ferrocenyl(biphenyl)platinum(II) compound, Fe(η^5-$C_5H_4PPh_2$)$_2$Pt(bph), its X-ray structure, and its physical and photophysical properties.

Experimental Section

Materials. Pt(bph)(CO)$_2$ was prepared as reported earlier.[7] 1,1′-Bis(diphenylphosphino)ferrocene, Fe(η^5-$C_5H_4PPh_2$)$_2$, was purchased from Aldrich (98%) and used as received. Tetrabutylammonium hexafluorophosphate (TBAH) was electrometric grade and purchased from SACHEM. Methylene chloride and methanol were optima grade and purchased from Fisher Scientific. Absolute ethanol was obtained from McCormick Distilling Co. Mixed solvents of 4:1 (v/v) C_2H_5OH/CH_3OH were used in studies at 77 K.

Synthesis of Fe(η^5-$C_5H_4PPh_2$)$_2$Pt(bph). Pt(bph)(CO)$_2$ (0.1753 g, 0.4347 mmol) and Fe(η^5-$C_5H_4PPh_2$)$_2$ (0.2892 g, 0.5216 mmol) were introduced into a 100 mL round-bottomed flask containing 50 mL of CH_2Cl_2. The reaction mixture was stirred at room temperature, and bubbles of CO were observed as the reaction proceeded. The dark green colored Pt(bph)(CO)$_2$ solid gradually reacted with Fe(η^5-$C_5H_4PPh_2$)$_2$, producing an orange-yellow precipitate over a period of 4 h. After 7 h, the resultant mixture was filtered and washed with cold CH_2Cl_2. The yield of the solid was 0.22 g (56%). The IR spectrum of the compound in KBr showed no absorption at either 2120 or 2092 cm^{-1}, where CO in Pt(bph)(CO)$_2$ absorbs. Crystals were then grown in a mixed solvent of CH_2Cl_2 and CH_3OH for single-crystal X-ray and photophysical studies.

Physical Measurements. IR spectra were recorded with a Perkin-Elmer model 1600 FT-IR. UV−visible spectra were recorded with a double-beam OLIS CARY 14 spectrophotometer, and spectra were measured at 296 K for samples dissolved in CH_2Cl_2 and 4:1 (v/v) C_2H_5OH/CH_3OH. Electrochemical measurements were performed at 296 K with a model 263 EG&G potentiostat/galvanostat contolled by model 270 electrochemistry software. A standard three-electrode system was employed with a platinum disk as the working electrode. A Pt wire was the counter electrode, and Ag/AgCl in 0.1 M TBAH CH_3CN served as the reference electrode. Measurements were carried out in CH_2Cl_2 containing 0.1 M TBAH as the supporting electrolyte. The ferrocenium/ferrocene couple (0.4 V)[10] was used as an internal reference. The scan rate was 50 mV s^{-1}.

[†] Wichita State University.
[‡] Texas A & M University.

(1) Clemente, D. A.; Pilloni, G.; Corain, B.; Longato, B.; Tiripicchio-Camellini, M. *Inorg. Chim. Acta* **1986**, *115*, L9.
(2) Butler, I. R. *Organometallics* **1992**, *11*, 74.
(3) Beer, P. D.; Kocian, O.; Mortimer, R. J. *J. Chem. Soc., Dalton, Trans.* **1990**, 3283.
(4) Zheng, G. Y.; Rillema, D. P. *Inorg. Chem.* **1998**, *37*, 1392.
(5) DePriest, J.; Zheng, G. Y.; Woods, C.; Rillema, D. P.; Mikirova, N. A.; Zandler, M. E. *Inorg. Chim. Acta* **1997**, *264*, 287.
(6) Chen, Y.; Woods, C.; Perkovic, M. W.; Rillema, D. P. *J. Chem. Crystallogr.* **1996**, *26*, 527.
(7) Chen, Y.-H.; Merkert, J. W.; Murtaza, Z.; Woods, C.; Rillema, D. P. *Inorg. Chim. Acta* **1995**, *240*, 41.
(8) Blanton, C. B.; Murtaza, Z.; Shaver, R. J.; Rillema, D. P. *Inorg. Chem.* **1992**, *31*, 3230.
(9) Blanton, C. B.; Rillema, D. P. *Inorg. Chim. Acta* **1990**, *168*, 145.

10.1021/ic980549n CCC: $18.00 © 1999 American Chemical Society
Published on Web 02/04/1999

Emission spectra were recorded with a Spex Fluorolog 212 spectrofluorometer equipped with double monochromator and a PMT (R928 Hamamatsu) as the detector. Excitation and emission spectra for samples dissolved in CH_2Cl_2 and 4:1 (v/v) C_2H_5OH/CH_3OH were measured at 296 and 77 K and corrected for instrument response. Samples in CH_2Cl_2 were degassed by bubbling Ar through the sample solution for 30 min prior to measurement. Samples in 4:1 (v/v) C_2H_5OH/CH_3OH were degassed by at least three freeze−pump−thaw cycles prior to measurement.

Excited-state lifetimes were measured at 77 K by exciting the sample at 355 nm with a frequency-tripled Nd:YAG laser (Continuum Surlite, run at ≤ 1.5 mJ/10 ns pulse). Spectra regions were isolated with a Hamamatsu R955 PMT in a cooled housing (−15 °C, Amherst) coupled to an Acton SpectraPro 275 monochromator. Transients were recorded with a LeCroy 9359A digital oscilloscope (1 Gs/s). Oscilloscope control and data curve fitting were accomplished with a program developed in-house.

X-ray Single-Crystal Structure Measurements. A red-yellow plate of Fe(η^5-$C_5H_4PPh_2$)$_2$Pt(bph) was mounted on a glass fiber at room temperature. Preliminary examination and data collection was performed on a Rigaku AFC5 (oriented graphite monochromator; Cu Kα radiation, $\lambda = 1.5418$ Å) at 203(2) K.[11] Cell parameters were calculated from the least-squares fitting for 25 high-angle reflections ($2\theta > 40°$). Omega scans for several intense reflections indicated acceptable crystal quality.

Data were collected from 6.32° to 120.14° 2θ at 203(2) K. The scan width for data collection was $1.54 + 0.3 \tan\theta°$ in omega with a fixed scan rate of 16.0 deg/min. Weak reflections were rescanned (maximum of two rescans), and the counts for each scan were accumulated. The three standards, collected every 150 reflections, showed no significant trends. Background measurements were made by stationary crystal and stationary counter techniques at the beginning and the end of each scan for half the total scan time.

Lorentz and polarization corrections were applied to 7155 reflections. A semiempirical absorption correction was applied. A total of 4559 unique reflections ($R_{int} = 0.0596$) with $I \geq 2\sigma(I)$ were observed. The structure was solved by direct methods.[12] Full-matrix least-squares anisotropic refinement for all non-hydrogen atoms yielded $R(F)$ [$I \geq 2\sigma(I)$] = 0.071 and $wR(F^2)$ [$I \geq 2\sigma(I)$] = 0.177 at convergence.[13] Hydrogen atoms were placed in idealized positions, with isotropic thermal parameters fixed at 1.5 times the attached atom. Neutral atom scattering factors and anomalous scattering factors were taken from the International Tables for X-ray Crystallography, Vol. C. A summary of crystallographic data collection and refinement parameters for Fe(η^5-$C_5H_4PPh_2$)$_2$Pt(bph) is given in Table 1.

For Fe(η^5-$C_5H_4PPh_2$)$_2$Pt(bph)·$2CH_2Cl_2$, a suitable crystal was mounted on a glass fiber at room temperature. Preliminary examination and data collection were performed on a Siemens P4 single-crystal diffractometer (oriented graphite monochromator; Mo Kα radiation, $\lambda = 0.710\ 73$ Å) at 299(2) K. Cell parameters were calculated from the least-squares fitting for 25 high-angle reflections ($2\theta > 15°$). Omega scans for several intense reflections indicated acceptable crystal quality.

Data were collected from 4.32° to 50.02° 2θ at 299(2) K. Scan width for data collection was 2.0° in omega with a variable scan rate of 3°/min. The three standards, collected every 97 reflections, showed no significant trends. Background measurements were made by stationary crystal and stationary counter techniques at the beginning and end of each scan for half the total scan time.

Lorentz and polarization corrections were applied to 7853 reflections. A semiempirical absorption correction was applied. A total of 7734 unique observed reflections ($R_{int} = 0.0455$) were used in further calculations. The structure was solved by direct methods.[12] Full-matrix least-squares anisotropic <isotropic> refinement for all non-hydrogen atoms yielded $R(F)$ [$I > 2\sigma(I)$] = 0.078 and $wR(F^2)$ [$I > 2\sigma(I)$] = 0.0856 at convergence.[13] Two methylene chloride molecules of solvation were located in the asymmetric area of the unit cell. One of the two solvents indicated positional disorder of a chlorine atom. The disordered chlorine atom of the solvent was modeled between two sites of 64% and 36% occupation, respectively. Hydrogen atoms were placed in idealized positions, with isotropic thermal parameters riding on the adjacent carbon atom thermal parameters. Neutral atom scattering factors and anomalous scattering factors were taken from the International Tables for X-ray Crystallography, Vol. C. A summary of crystallographic data collection and refinement parameters for Fe(η^5-$C_5H_4PPh_2$)$_2$Pt(bph)·$2CH_2Cl_2$ is given in Table 1.

Table 1. Crystal and Structure Refinement Data for Fe($C_5H_4PPh_2$)$_2$Pt(bph) (**1**) and Fe($C_5H_4PPh_2$)$_2$Pt(bph)·$2CH_2Cl_2$ (**2**)

	1	**2**
formula	$C_{46}H_{36}FeP_2Pt$	$C_{48}H_{40}Cl_2FeP_2Pt$
fw	901.6	1071.48
T (K)	203(2)	299(2)
λ	1.5418	0.710 73
cryst syst	triclinic	monoclinic
space group	$P1$	$P2_1/n$
a (Å)	9.777(2)	12.698(3)
b (Å)	18.003(4)	14.161(3)
c (Å)	20.882(4)	23.376(6)
α (deg)	93.57(3)	90
β (deg)	100.99(30)	94.107(14)
γ (deg)	90.86	90
V (A^3)	3600(1)	4192.5(18)
Z	4	4
ρ_{calcd} (g/cm^{-1})	1.664	1.698
μ (mm^{-1})	11.481	4.045
R1[a]	0.0705	0.0458
wR2[a]	0.1755	0.0856

[a] $R1 = \sum(|F_o| - |F_c|/|F_o|$ and $wR2 = (\sum w(F_o^2 - F_c^2)^2/\sum w(F_o^4)^{1/2}$.

Table 2. Selected Bond Lengths (Å) and Angles (deg) for (Fe($C_5H_4PPh_2$)$_2$Pt(bph) (**1**) and (Fe($C_5H_4PPh_2$)$_2$Pt(bph)·$2CH_2Cl_2$ (**2**)

1		**2**	
Pt(1A)−C(1A)	2.07(2)	Pt(1)−C(1)	2.076(7)
Pt(1A)−C(12A)	2.08(2)	Pt(1)−C(12)	2.066(7)
Pt(1A)−P(1A)	2.340(7)	Pt(1)−P(1)	2.316(2)
Pt(1A)−P(2A)	2.338(5)	Pt(1)−P(2)	2.319(2)
Fe(1A)−C(13A)	1.96(2)	Fe(1)−C(13)	2.002(7)
Fe(1A)−C(14A)	2.03(2)	Fe(1)−C(14)	2.034(9)
Fe(1A)−C(15A)	2.01(2)	Fe(1)−C(15)	2.049(8)
Fe(1A)−C(16A)	2.04(2)	Fe(1)−C(16)	2.044(9)
Fe(1A)−C(17A)	2.02(2)	Fe(1)−C(17)	2.024(8)
C(1A)−C(2A)	1.40(2)	C(1)−C(2)	1.395(10)
P(1A)−C(13A)	1.79(2)	P(1)−C(13)	1.816(8)
P(1A)−C(18A)	1.82(2)	P(1)−C(18)	1.816(8)
P(1A)−C(24A)	1.85(2)	P(1)−C(24)	1.827(7)
Fe(1A)−Pt(1A)	4.24(4)[a]	Fe(1)−Pt(1)	4.378(1)[a]
C(12A)−Pt(1A)−P(1A)	168.9(6)	C(12)−Pt(1)−P(2)	165.8(2)
P(2A)−Pt(1A)−P(1A)	98.3(2)	P(2)−Pt(1)−P(1)	98.61(7)
C(1A)−Pt(1A)−C(12A)	81.1(7)	C(1)−Pt(1)−C(12)	80.1(3)
C(1A)−Pt(1A)−P(1A)	92.2(5)	C(1)−Pt(1)−P(2)	92.8(2)
C(1A)−Pt(1A)−P(2A)	167.2(6)	C(1)−Pt(1)−P(1)	162.6(2)
C(12A)−Pt−P(2A)	89.7(5)	C(12)−Pt−(1)	91.3(2)

[a] The distance between these two atoms was calculated from the atomic coordinates.

Results

X-ray Structure. Selected bond lengths and angles of [Fe(η^5-$C_5H_4PPh_2$)$_2$Pt(bph)] and Fe(η^5-$C_5H_4PPh_2$)$_2$Pt(bph)·$2CH_2Cl_2$ are given in Table 2. ORTEP drawings of [Fe(η^5-$C_5H_4PPh_2$)$_2$-Pt(bph)] and Fe(η^5-$C_5H_4PPh_2$)$_2$Pt(bph)·$2CH_2Cl_2$ are given in Figure 1. The structures were distorted from square planar geometry as noted by the Pt−C bond lengths of 2.07 Å, the

(10) Bard, A. J.; Faulkner, L. R. *Electrochemical Methods*; Wiley: New York, 1980; and references therein.
(11) *MSC CTR(PC)*. Program for reduction for Rigaku AFC5 diffractometer control; Molecular Structures Corp.: Woodlands, TX, 1995.
(12) Sheldrick, G. *SHELXS-86*. Program for Crystal Structure Solution; Institut für Anorganische Chemie der Universitat: Tammanstrasse 4, D-3400 Gottingen, Germany, 1986.
(13) Sheldrick, G. *SHELXL-93*. Program for Crystal Structure Refinement; Institut für Anorganische Chemie der Universitat: Tammanstrasse 4, D-3400 Gottingen, Germany, 1993.

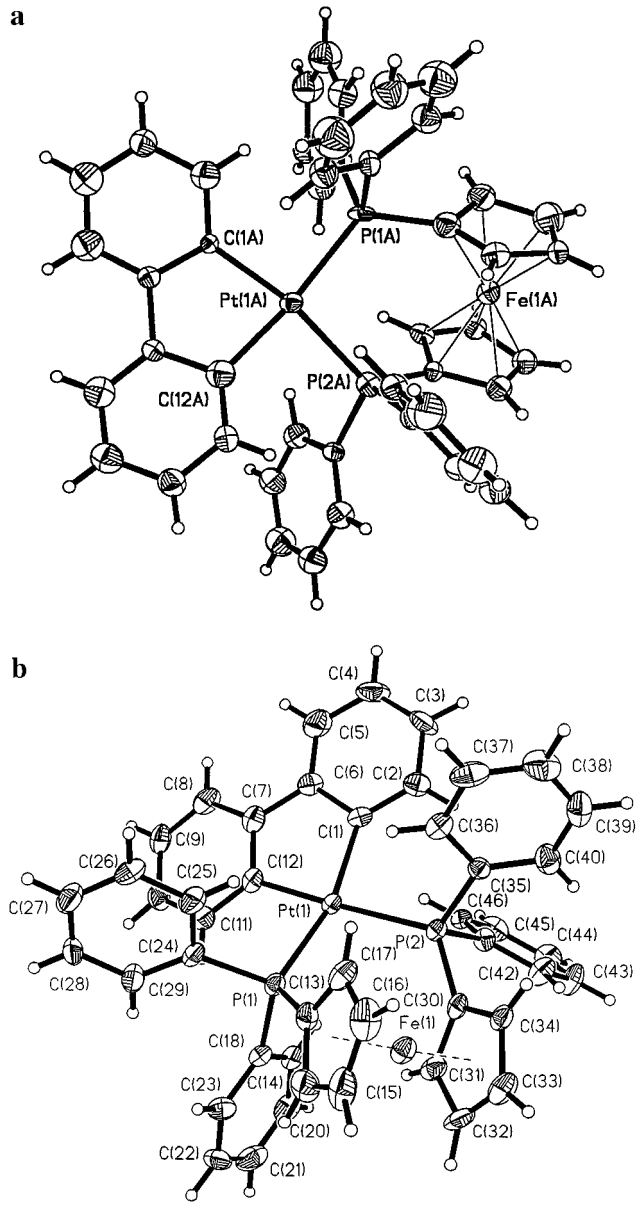

Figure 1. Crystal structure of Fe(η^5-$C_5H_4PPh_2$)$_2$Pt(bph) (a) and Fe(η^5-$C_5H_4PPh_2$)$_2$Pt(bph)·2CH_2Cl_2 (b).

Pt−P bond lengths of 2.32 Å, the C−Pt−P (P trans to C) angle of 162.6−168.9°, the C−Pt−P (P cis to C) angle of 89.7−92.8°, the C−Pt−C angle of 80.1−81.1°, and the P−Pt−P angle of 98.6°. The cyclopentadienyl rings (Cp) are in a staggered conformation. The distance between Pt and Fe was 4.24 Å for [Fe(η^5-$C_5H_4PPh_2$)$_2$Pt(bph)] and 4.38 Å for Fe(η^5-$C_5H_4PPh_2$)$_2$-Pt(bph)·2CH_2Cl_2 as calculated from their atomic coordinates.

Electrochemistry. Figure 2 shows the cyclic voltammograms for [Fe(η^5-$C_5H_4PPh_2$)$_2$Pt(bph)] (top) and Fe(η^5-$C_5H_4PPh_2$)$_2$ (bottom). Fe(η^5-$C_5H_4PPh_2$)$_2$ was present in both solutions and showed reversible behavior, but the oxidation potential for the ferrocene moiety in [Fe(η^5-$C_5H_4PPh_2$)$_2$Pt(bph)] displayed only quasireversible behavior. Its peak anodic current shifted positively from 0.63 V for Fe(η^5-$C_5H_4PPh_2$)$_2$ to 0.76 V for [Fe(η^5-$C_5H_4PPh_2$)$_2$Pt(bph)].

Photophysical Properties. The UV absorption spectra of Fe(η^5-$C_5H_4PPh_2$)$_2$ and [Fe(η^5-$C_5H_4PPh_2$)$_2$Pt(bph)] are shown in Figure 3. Transitions at 286 and 442 nm were observed for Fe(η^5-$C_5H_4PPh_2$)$_2$. The former is assigned as a $\pi \rightarrow \pi^*$ transition associated with the phenyl group, and latter is assigned as a

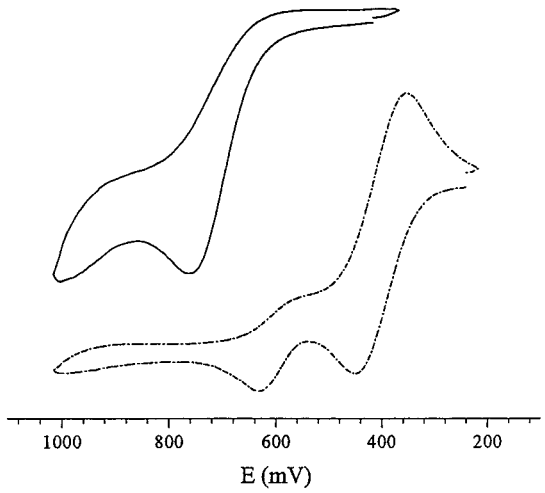

Figure 2. Cyclic voltammogram of Fe(η^5-$C_5H_4PPh_2$)$_2$Pt(bph) in CH_2Cl_2 containing 0.1 M TBAH at 296 K. Pt as working electrode, Ag/AgCl in 0.1 M TBAH CH_3CN as reference electrode. Scan rate 50 mV s^{-1}. (—) Fe(η^5-$C_5H_4PPh_2$)$_2$Pt(bph). (— · —) Fe(η^5-$C_5H_4PPh_2$)$_2$ containing Fe(η^5-C_5H_5)$_2$.

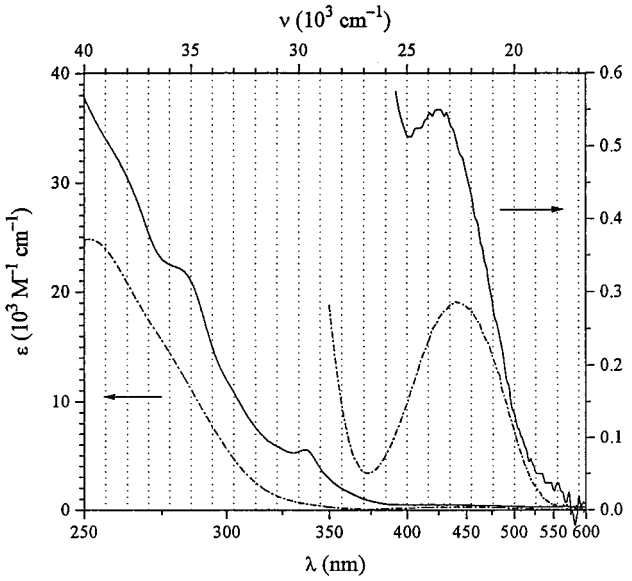

Figure 3. UV−vis absorption spectra in CH_2Cl_2 at 296 K. (—) Fe(η^5-$C_5H_4PPh_2$)$_2$Pt(bph). (— · —) Fe(η^5-$C_5H_4PPh_2$)$_2$.

dπ(Fe) → π^*(Cp) MLCT transition. Upon coordination, the dπ-(Fe) → π^*(Cp) MLCT band blue shifted to 425 nm, whereas the band at 286 nm simply became a shoulder on the $\pi \rightarrow \pi^*$-(bph) transition. In addition, a band centered at 337 nm was observed and assigned as a dπ(Pt) → π^*(bph) MLCT transition by analogy with a similar assignment for Pt(bph)(dppm).[5]

Excitation at the dπ(Pt) → π^*(bph) transition in a 4:1 C_2H_5-OH/CH_3OH glass at 77 K resulted in the highly structured emission spectrum shown in Figure 4. Upon warming to 296 K, no resolved emission was seen. Compared to Pt(bph)(dppm), the excited-state lifetime at 77 K decreased from 16 to 6 μs, but the emission energy maximum increased from 19 650 to 20 000 cm^{-1}. Photophysical data are collected in Table 3.

Discussion

X-ray Structure. The Pt−C (bph) bond length of 2.07 Å is slightly longer than those (2.01−2.04 Å) reported for the other Pt(bph) derivatives.[6,7] This increase in the Pt−C bond length can be explained by changes in the anchillary ligands, since

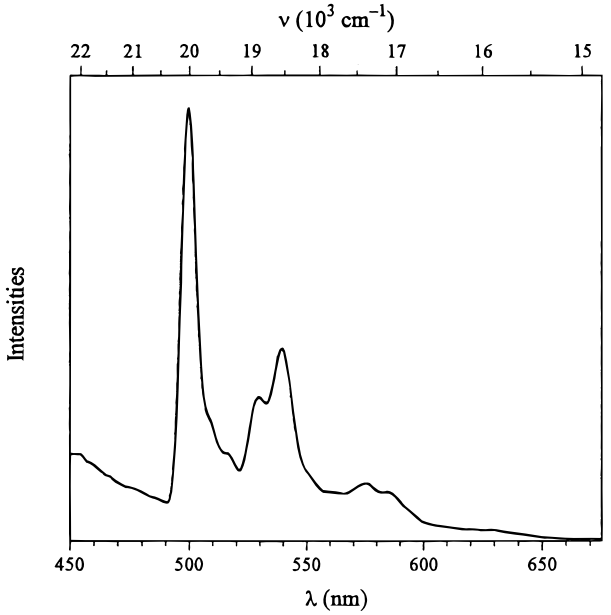

Figure 4. Emission spectra of Fe(η^5-$C_5H_4PPh_2$)$_2$Pt(bph) in 4:1 (v/v) C_2H_5OH/CH_3OH at 77 K, excited at 355 nm.

Table 3. Excited-State Properties of Fe(η^5-$C_5H_4PPh_2$)$_2$Pt(bph) in 4:1 (v/v) C_2H_5OH/CH_3OH at 77 K

compound	UV absorption[a] (nm)	$E_{em,max}$ (10^3 cm^{-1})	τ (ms)
Fe(η^5-$C_5H_4PPh_2$)$_2$Pt(bph)	337	20.00	6.17 ± 0.30
Pt(bph)(dppm)[5]	345	19.65	16.7 ± 1.4

[a] UV absorption was measured in CH_2Cl_2 at 296 K.

Fe(η^5-$C_5H_4PPh_2$)$_2$ is not as good a π acceptor ligand as CO[7] or COD[6] (COD = 1,5-cyclooctadiene). The bond length is comparable to 2.09 Å found for Pt−C in (7,8-bzq)Pt(dppm), where 7,8-bzq = 7,8-benzoquinoline and dppm = bis(diphenylphosphino)methane).[6] The Pt−P bond length of 2.34 Å is longer than the Pt−P bond length of 2.25 Å reported for [Fe(η^5-$C_5H_4PPh_2$)$_2$Pt(Cl)$_2$].[1] The increase in Pt−P bond length can be attributed to the stronger π acceptor properties of the bph ligand. The C−Pt−C (bph) angle of 81.1−92.8° is slightly larger than that of 79.2° for (COD)Pt(bph) and 80.5° for (CO)$_2$Pt(bph). The P−Pt−P angle of 98.6° is slightly smaller than that of 99.3° for Fe(η^5-$C_5H_4PPh_2$)$_2$Pt(Cl)$_2$, but larger than the P−Pt−P bite angles of 72.1°, 84.5°, and 91.6° for the series Pt(7,8-bzq)(dppm), Pt(7,8-bzq)(dppe), and Pt(7,8-bzq)(dppp), where dppm = 1,2-bis(diphenylphosphino)methane, dppe = 1,2-bis(diphenylphosphino)ethane and dppp = 1,3-bis(diphenylphosphino)propane. The larger P−Pt−P bite angle is attributed to the larger size of Fe(η^5-$C_5H_4PPh_2$)$_2$ compared to either dppm, dppe, or dppp. The distance between Pt and Fe of 4.24 Å for Fe(η^5-$C_5H_4PPh_2$)$_2$Pt(bph) and 4.38 Å for Fe(η^5-$C_5H_4PPh_2$)$_2$Pt(bph)·2CH_2Cl_2 is comparable to the Pt−Fe distance of 4.28 Å reported for [Fe(η^5-$C_5H_4PPh_2$)$_2$Pt(Cl)$_2$].[1]

Electrochemistry. As shown in Figure 2, oxidation of the ferrocenyl moiety in Fe(η^5-$C_5H_4PPh_2$)$_2$Pt(bph) was irreversible and the anodic potential shifted positively by +0.13 V compared to Fe(η^5-$C_5H_4PPh_2$)$_2$. The irreversibility can be attributed to strong bonding with the biphenyl ligand, which functions as both a good electron donor and acceptor. Since Cl^- serves as an electron donor but a weak electron acceptor, less electron interaction between Pt and Cl^- is expected. The increase in difficulty to remove an electron from the ferrocenyl moiety is attributed to redistribution of the electron density from the ferrocene unit to the Pt unit resulting from coordination with Pt(II). The shift of the electron density toward the Pt(II) center makes the Fe(II) center more difficult to oxidize. The anodic potential of 0.63 V agreed well with the reported anodic potential of 0.60 V for the ferrocenyl moiety in [Fe(η^5-$C_5H_4PPh_2$)$_2$Pt(Cl)$_2$].[1]

Photophysical Properties. The blue shift of the MLCT dπ(Fe) → π^*(Cp) band for Fe(η^5-$C_5H_4PPh_2$)$_2$Pt(Cl)$_2$ relative to that for Fe(η^5-$C_5H_4PPh_2$)$_2$ agrees with the observed positive shift of the anodic potential. The blue shift from 442 to 425 nm corresponds to an increase in energy of 0.11 eV, while the change of anodic potential in energy was 0.13 eV. Similarly, the MLCT dπ(Pt) → π^*(bph) band at 337 nm for Fe(η^5-$C_5H_4PPh_2$)$_2$Pt(bph) was blue shifted compared to Pt(bph)(dppm), which was observed at 345 nm.

At 77 K, Fe(η^5-$C_5H_4PPh_2$)$_2$Pt(bph) showed structured emission similar to Pt(bph)(dppm), but was blue shifted. This result agrees with the changes observed for the UV absorption spectra. The similarity of the emission profile and its vibronic progression to that of Pt(bph)(dppm) leads to the assignment of the emitting state as a metal-perturbed bph-centered ^{3}LC state. The excited-state lifetime of 6.17 μs at 77 K is shorter compared to that of 16.7 μs for Pt(bph)(dppm), although it would be expected to be longer according to energy gap law. The shorter lifetime can be attributed to quenching of the emitting state by the ferrocenyl moiety. The process can be expressed by eqs 1 and 2. According to eq 2, the emitting state is quenched via electron

$$Fe^{II}(\eta^5\text{-}C_5H_4PPh_2)_2Pt^{II}(bph) \xrightarrow{h\nu} Fe^{II}(\eta^5\text{-}C_5H_4PPh_2)_2Pt^{III}(bph^{\bullet -}) \quad (1)$$

$$Fe^{II}(\eta^5\text{-}C_5H_4PPh_2)_2Pt^{III}(bph^{\bullet -}) \rightarrow Fe^{III}(\eta^5\text{-}C_5H_4PPh_2)_2Pt^{II}(bph^{\bullet -}) \quad (2)$$

transfer from the Fe^{II} center to the Pt^{III} center, forming a charge-separated species. This process is greatly enhanced as the temperature increased to 296 K, where no emission is observed, in contrast to Pt(bph)(dppm), where pronounced emission is found, even at room temperature.

Conclusion

A chromophore-electroactive quencher compound, Fe(η^5-$C_5H_4PPh_2$)$_2$Pt(bph), has been synthesized. The emitting state, which has been assigned as a bph-centered ^{3}LC state, was quenched by the ferrocenyl moiety via an electron-transfer mechanism. The emitting state lifetime was shorter than that for Pt(bph)(dppm) at 77 K and too short to be detected with a nanosecond laser system at 296 K.

Acknowledgment. We thank the Office of Basic Energy Sciences of the Department of Energy for support, the National Science Foundation for the laser equipment, and Johnson-Matthey for the source compound on loan.

Supporting Information Available: Tables S1−5 for Fe(η5-$C_5H_4PPh_2$)2Pt(bph) and Tables S6−10 for Fe(η5-$C_5H_4PPh_2$)2Pt(bph)·2CH_2Cl_2, listing crystallographic and refinement data, atomic coordinates and isotropic displacement parameters, complete bond distances and coordinates, and anisotropic displacement parameters and hydrogen coordinates. This material is available free of charge via the Internet at http://pubs.acs.org.

IC980549N